

A DFT and ^{59}Co Solid-State NMR Study of the Second-Sphere Interaction in Polyammonium Macrocyclic Cobalt Cyanide Supercomplexes

Ping Zhou, Steve C. F. Au-Yeung,* and Xiao-Ping Xu

Contribution from the Department of Chemistry, The Chinese University of Hong Kong, Shatin, New Territories, Hong Kong

Received June 2, 1998. Revised Manuscript Received October 26, 1998

Abstract: The second-sphere interaction for a series of supercomplexes formed from the binding of $[\text{Co}(\text{CN})_6]^{3-}$, a photochemical active metal complex, with preorganized protonated polyammonium macrocyclics has been studied with ^{59}Co solid-state NMR and ab initio quantum chemical methods at the DFT level. For the supercomplexes studied in this work, the ^{59}Co NMR chemical shift of $[\text{Co}(\text{CN})_6]^{3-}$ has been successfully computed, demonstrating that the hybrid XC functional method is equally powerful in rationalizing small adjustments in structural and electronic modification at the metal center. This success has confirmed that the entire ^{59}Co chemical shift range may be predicted with reasonable confidence. The charge-transfer mechanism has also been established on the basis of the correlations between the ^{59}Co chemical shifts and the relative contribution of cobalt-3d orbitals to second-order interaction energies, as well as structure parameters. The shielding tensor results confirmed that the structure distortions occurring in these supercomplexes are the direct consequence of the second-sphere interaction resulting from site-symmetry being lowered at cobalt. Thus, the degeneracy of the electron energy state ($^1\text{T}_{1g}$) at cobalt has been lifted, resulting in splitting of the energy levels.

Introduction

The use of density functional theory (DFT) as an efficient alternative to the post-Hartree–Fock methods in the ab initio computation of NMR chemical shifts has gained significant grounds since the pioneering DFT-IGLO (individual gauge for localized orbitals) study of Malkin *et al.*,¹ and the GIAO (gauge including atomic orbitals) approach by Schreckenbach and Ziegler.² Although past efforts have been focused on lighter elements, recent activities have focused on the study of transition metals using DFT method.^{1b,3–6} The impetus for this quest is based on the belief that NMR chemical shielding tensors can facilitate in depth understanding in structure, bonding and potentially “functional” issues in catalysis, ligand binding in biological systems, and photochemical processes. Recent applications of the natural bond orbital (NBO) analysis have also been successful in the study of the electronic structure in various

metal systems such as group IIIA metal oxides,⁷ hexamethyltungsten,⁸ and pentaaminecobalt(III) complexes.⁹ Although past endeavor has focused on methodology development for the prediction of ^{59}Co chemical shifts spanning the entire chemical shift range (app. 15 000 ppm) whereby large structural or electronic structure changes is involved,^{4b,5} it remains unclear if the same methodology is equally suitable for the prediction of small changes in the ^{59}Co chemical shifts resulting from small adjustment in either of these two factors at the metal center. This issue forms one of the objectives of this study and is expected to be a commonly encountered situation whereby “structure–function” properties of a ligand system may be fine-tuned through small systematic adjustments as in the binding of protonated polyammonium macrocyclic ions to photochemical active metal complex anions^{10,11} or in synthetic metalloporphyrin systems.¹²

Another application of DFT method to be explored in this study is its use in the study of second-sphere interaction involving the binding of photochemical active metal complex anions with protonated polyammonium macrocyclics and their charge-transfer mechanism, which forms an important basis in molecular self-assembly, recognition, and photochemistry of

* To whom correspondence should be addressed. E-mail: scfauyeung@cuhk.edu.hk.

(1) (a) Malkin, V. G.; Malkina, O. L.; Salahub, D. R. *Chem. Phys. Lett.* **1993**, *204*, 80. (b) Malkin, V. G.; Malkina, O. L.; Casida, M. K.; Salahub, D. R. *J. Am. Chem. Soc.* **1994**, *116*, 5898–5980. (c) Malkin, V. G.; Malkina, O. L.; Eriksson, L. A.; Salahub, D. R. In *Theoretical and Computational Chemistry*; Politzer, P., Seminario, J. M., Eds.; Amsterdam, 1995; Vol. 2.

(2) (a) Schreckenbach G.; Ziegler, T. *J. Phys. Chem.* **1995**, *99*, 606–611. (b) Schreckenbach G.; Ziegler, T. *Int. J. Quantum Chem.* **1996**, *60*, 753.

(3) (a) Bühl, M. *J. Phys. Chem. A* **1997**, *101*, 2514–2517. (b) Bühl, M. *Chem. Phys. Lett.* **1997**, *267*, 251–257. (c) Bühl, M. *Organometallics* **1997**, *16*, 261. (d) Bühl, M. *Angew. Chem., Int. Ed. Engl.* **1998**, *37*, 142–144.

(4) (a) Chan, J. C. C.; Au-Yeung, S. C. F. *J. Mol. Struct. (THEOCHEM)* **1997**, *393*, 93–96. (b) Chan, J. C. C.; Au-Yeung, S. C. F. *J. Phys. Chem. A* **1997**, *101*, 3638–3640.

(5) Godbout, N.; Oldfield, E. *J. Am. Chem. Soc.* **1997**, *119*, 8065–8069.

(6) Ruiz-Morales, Y.; Ziegler, T. *J. Phys. Chem. A* **1998**, *102*, 3970–3976.

(7) (a) Nemukhin, A. V.; Weinhold, F. *J. Chem. Phys.* **1992**, *97*, 3420.

(b) Nemukhin, A. V.; Weinhold, F. *J. Chem. Phys.* **1993**, *98*, 1329.

(8) (a) Lledos, A.; Suades, J.; Alvarez-Larena, A.; Piniella, J. F. *Organometallics* **1995**, *14*, 1053. (b) Kaupp, M. *J. Am. Chem. Soc.* **1996**, *118*, 3018.

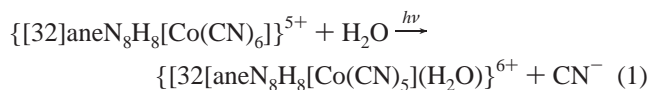
(9) Chan, J. C. C.; Au-Yeung, S. C. F. *J. Phys. Chem. A* **1997**, *101*, 4196–4201.

(10) Manfrin, M. E.; Sabatini, N.; Moggi, L.; Balzani, V.; Hosseini, M. W.; Lehn, J. M. *J. Chem. Soc., Chem. Commun.* **1984**, 555.

(11) Manfrin, M. F.; Moggi, L.; Castelvetro, V.; Balzani, V.; Hosseini, M. W.; Lehn, J. M. *J. Am. Chem. Soc.* **1985**, *107*, 6888–6892.

(12) Bang, H.; Edeards, J. O.; Kim, J.; Lawler, R. G.; Reynolds, K.; Ryan, W. J.; Sweigart, D. A. *J. Am. Chem. Soc.* **1992**, *114*, 2843–2852.

supercomplexes.^{13–18} For example, it has been established that $\{[32]\text{aneN}_8\text{H}_8[\text{Co}(\text{CN})_6]\}^{5+}$ undergoes photoaquation when irradiated at 313 nm¹¹



Because the observed spectral changes are qualitatively identical with those obtained from the photoaquation of “free” $[\text{Co}(\text{CN})_6]^{3-}$ when its ${}^1\text{A}_{1g} \rightarrow {}^1\text{T}_{1g}$ transition at 313 nm is irradiated,^{19,20} it has been assumed¹¹ that $\{[32]\text{aneN}_8\text{H}_8[\text{Co}(\text{CN})_6]\}^{5+}$ undergoes the same photoaquation reaction in the form of free $[\text{Co}(\text{CN})_6]^{3-}$ as observed in the reaction



A considerable reduction of the photoaquation quantum yield (ϕ) was found for $\{[24]\text{aneN}_6\text{H}_6[\text{Co}(\text{CN})_6]\}^{5+}$ ($\phi = 0.15$) and $\{[32]\text{aneN}_8\text{H}_8[\text{Co}(\text{CN})_6]\}^{5+}$ ($\phi = 0.1$) when compared with free $[\text{Co}(\text{CN})_6]^{3-}$ ($\phi = 0.3$).¹¹ These observed changes in ϕ have been attributed to the geometrical encapsulation of the cyano groups by polyammonium macrocycles based on space-filling models.¹¹ However, X-ray crystal structure study of a series of similar supercomplexes^{21,22} has confirmed that the second-sphere interaction plays an important role in the stability of their structures but ruled out operation of all suggested encapsulation models proposed earlier.¹¹ Thus, the supercomplexes $\{[18]\text{aneN}_6\text{H}_2[\text{Co}(\text{CN})_6]\}^{5+}$ (1), $\{[16]\text{aneN}_4\text{H}_2[\text{Co}(\text{CN})_6]\}^{5+}$ (2), and $\{[12]\text{aneN}_4\text{H}_2[\text{Co}(\text{CN})_6]\}^{5+}$ (3), in which the single-crystal structure has been determined by us,²¹ form a unique group of compounds for probing the second-sphere interaction through a combined study of the solid-state ${}^{59}\text{Co}$ NMR together with the ab initio ${}^{59}\text{Co}$ chemical shift calculation and NBO analysis at DFT level. For the supercomplexes $\{[24]\text{aneN}_8\text{H}_6[\text{Co}(\text{CN})_6]\}^{5+}$ (5), $\{[24]\text{aneN}_6\text{H}_6[\text{Co}(\text{CN})_6]\}^{5+}$ (6), and $\{[32]\text{aneN}_8\text{H}_8[\text{Co}(\text{CN})_6]\}^{5+}$ (7), whereby the single-crystal structure is unavailable, they serve as an extension of the above study whereas $\text{K}_3[\text{Co}(\text{CN})_6]^{3-}$ (4) is also included for comparison.

Experimental Section

Materials. The polyammonium macrocycles $[18]\text{aneN}_6$, $[16]\text{aneN}_4$, $[12]\text{aneN}_4$, $[24]\text{aneN}_8$, $[24]\text{aneN}_6$, and $[32]\text{aneN}_8$ (Figure 1) were synthesized by following literature method.²³ Reagent grade potassium hexacyanocobaltate was purchased from E-Merck and was used without further purification. The supercomplexes²⁴ $\{[18]\text{aneN}_6\text{H}_2[\text{Co}(\text{CN})_6]\}^{5+}$

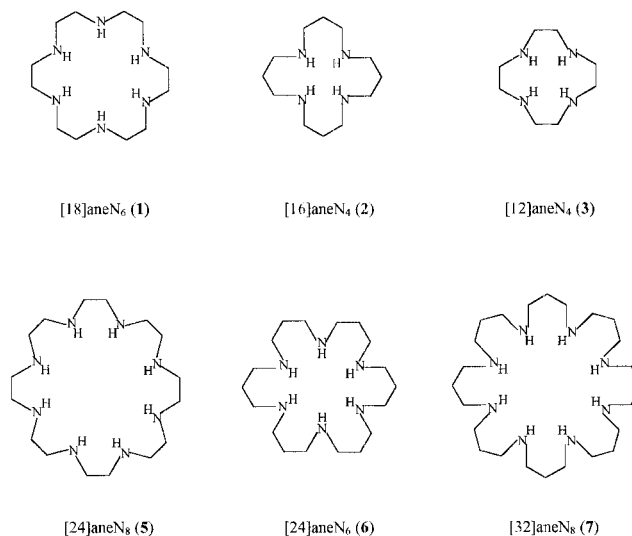


Figure 1. Schematic diagram of polyammonium macrocycles.

(1), $\{[16]\text{aneN}_4\text{H}_2[\text{Co}(\text{CN})_6]\}^{5+}$ (2), $\{[12]\text{aneN}_4\text{H}_2[\text{Co}(\text{CN})_6]\}^{5+}$ (3), $\{[24]\text{aneN}_8\text{H}_6[\text{Co}(\text{CN})_6]\}^{5+}$ (5), $\{[24]\text{aneN}_6\text{H}_6[\text{Co}(\text{CN})_6]\}^{5+}$ (6), and $\{[32]\text{aneN}_8\text{H}_8[\text{Co}(\text{CN})_6]\}^{5+}$ (7) were synthesized as described earlier.²¹

Solid-State NMR. The solid-state ${}^{59}\text{Co}$ NMR powder spectra were recorded at room temperature on a Bruker ASX-300 and AMX-400 spectrometer operating at 71.2 and 94.9 MHz, respectively. An aqueous concentrated $\text{K}_3[\text{Co}(\text{CN})_6]$ solution contained in a 2-mm diameter glass ball was used as an external reference for the determination of the ${}^{59}\text{Co}$ NMR chemical shifts. The B_1 field strength (50–80 kHz at 71.2 MHz and 41 kHz at 94.9 MHz) was determined by measuring the $\pi/2$ pulse width of the aqueous $\text{K}_3[\text{Co}(\text{CN})_6]$.²⁵ One-pulse spectra were recorded at 94.9 MHz. Because of the deadline problem, a two-pulse Hahn echo²⁶ sequence ($\theta_1 - \tau_1 - 2\theta_1 - \tau_2$ -acquire) was used to obtain spectra at 71.2 MHz, where θ_1 (0.8–1.0 μs) is the pulse width; τ_1 (25.5 μs) and τ_2 (15.5 μs) are the delay times. The FIDs were Fourier transformed, starting from the echo top after appropriate left-shifting. For all of the measurements, a 16-step phase cycling was employed,²⁷ and the recycle delays were in the range 0.1–0.5 s.

Simulation of Line Shape for Static Spectra. The solid-state NMR spectra were calculated by using the SECQUAD program.²⁸ The program has been modified to incorporate a nonlinear iterative fitting routine and has been tested extensively in this laboratory. Note that the original Euler angle α has been replaced by $\alpha' = \alpha + 90^\circ$ in this modified program compared with the convention used in the original SECQUAD program.²⁸ The analysis of the powder pattern involves the variation of eight parameters. They are the chemical shift (CS) tensor components δ_{11} , δ_{22} , and δ_{33} ($\delta_{11} \geq \delta_{22} \geq \delta_{33}$) following literature convention;²⁸ the nuclear quadrupolar coupling constant, NQCC; the asymmetry parameter, η_Q , of the electric field gradient (EFG); and the three Euler angles α , β , γ relating the principal axis system (PAS) of the EFG and CS tensors. The initial parameters used for the simulation of the spectra were taken from Lourens et al.²⁹ In addition, the method of singularity position³⁰ was used to generate the initial guess for the principal components of the chemical shielding tensor. The experimental and simulated spectra at the two magnetic fields are displayed in Figure 2 for complexes 1–4, whereas for complexes 5–7 they are given in Supporting Information Figure S1. The corresponding interaction parameters are summarized in Table 1.

(25) Slichter, C. P. *Principles of Magnetic Resonance*; Springer-Verlag: Hong Kong 1991.

(26) Cheng, J. J.; Edwards, J. C.; Ellis, P. D. *J. Phys. Chem.* **1990**, *94*, 4, 553.

(27) Farrar, T. C.; Becker, E. D. *Pulse and Fourier Transform NMR*; Academic Press: New York, 1971.

(28) Wasylshen, R. E.; Penner, G. H.; Power, W. P. and Curtis, T. D. *J. Phys. Chem.* **1990**, *94*, 591.

(29) Lourens, J. A. J.; Reynhardt, E. C. *Phys. Stat. Sol. (a)* **1972**, *11*, 739.

(30) Baugher, J. F.; Taylor, P. C.; Oja, T.; Bray, P. J. *J. Chem. Phys.* **1969**, *50*, 4914.

(13) Lindsey, J. S. *New J. Chem.* **1990**, *15*, 153.

(14) Whitesides, G. M.; Mathias, J. P.; Seto, C. T. *Science* **1991**, *254*, 1312.

(15) Lehn, J. M. *Angew. Chem., Int. Ed. Engl.* **1990**, *29*, 1304.

(16) Lehn, J. M. *Science* **1988**, *260*, 1762.

(17) Lu, Q.; Motekaitis, R. J.; Reibenspies, J. J.; Martell, A. E. *Inorg. Chem.* **1995**, *34*, 4958.

(18) Koike, T.; Inoue, M.; Kimura, E.; Shiro, M. *J. Am. Chem. Soc.* **1996**, *118*, 3091.

(19) Moggi, L.; Bolletta, F.; Balzani, V.; Scandola, F. *J. Inorg. Nucl. Chem.* **1966**, *28*, 2589.

(20) Adamson, A. W.; Chiang, A.; Zinato, E. *J. Am. Chem. Soc.* **1969**, *91*, 5467.

(21) Zhou, P.; Xue, F.; Au-Yeung, S. C. F.; Xu, X.-P. *Acta Crystallogr. B*, in press.

(22) Bencini, A.; Bianchi, A.; Garcia-España, E.; Giusti, M.; Mangani, S.; Micheloni, M.; Orioli, P.; Paoletti, P. *Inorg. Chem.* **1987**, *26*, 3902–3907.

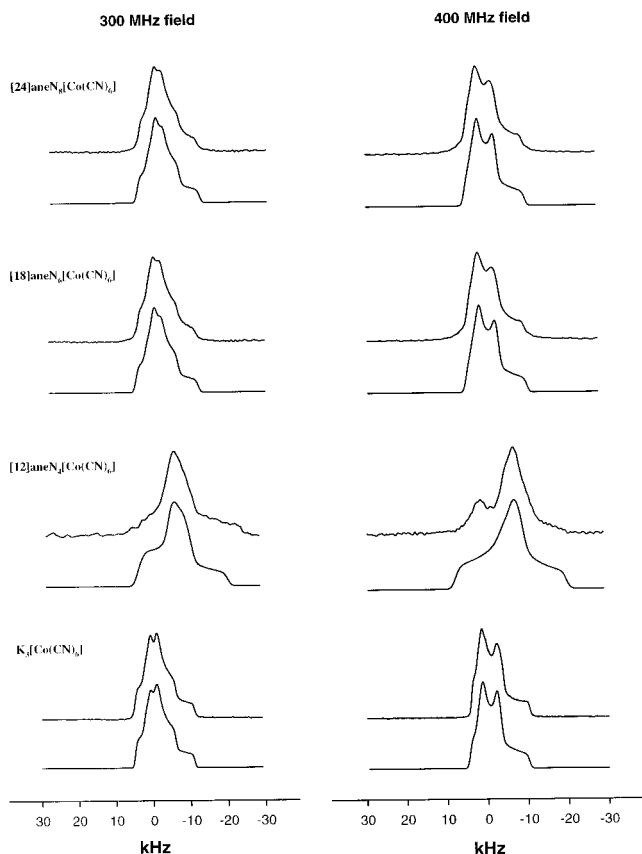
(23) Dietrich, B.; Hosseini, M. W.; Lehn, J.-M.; Sessions, R. B. *Helv. Chim. Acta* **1983**, *66*, 1262–1278. (b) Dietrich, B.; Hosseini, M. W.; Lehn, J. M.; Sessions, R. B. *J. Am. Chem. Soc.* **1981**, *103*, 1282.

(24) (a) Peter, F.; Gross, M.; Josseini, M. W.; Lehn, J. M. and Sessions, R. B. *Chem. Soc., Chem. Commun.* **1981**, 1067. (b) Peter, F.; Gross, M.; Hosseini, M. W. and Lehn, J. M. *Electroanal. Chem.* **1983**, *144*, 279.

Table 1. Simulated Parameters of Solid State ^{59}Co NMR Lineshape for Complexes 1–7

complex	δ_{11} (ppm)	δ_{22} (ppm)	δ_{33} (ppm)	δ_{iso}^a (ppm)	Ω^b (ppm)	NQCC ^c (MHz)	η_Q^d	α^e (deg)	β^e (deg)	γ^e (deg)
[18]aneN ₆ [Co(CN) ₆] (1)	86	84	-35	45	121	6.2	0.75	63	63	0
[16]aneN ₄ [Co(CN) ₆] (2)	53	30	-35	16	88	6.4	0.72	109	67	22
[12]aneN ₄ [Co(CN) ₆] (3)	80	-95	-170	-62	250	7.0	0.95	42	58	0
K ₃ [Co(CN) ₆] (4)	55	27	-40	15	96	6.2	0.82	106	66	14
[24]aneN ₈ [Co(CN) ₆] (5)	70	-30	-30	3	100	5.0	0.98	0	90	60
[24]aneN ₆ [Co(CN) ₆] (6)	188	51	-171	23	359	9.6	0.56	9	80	9
[32]aneN ₈ [Co(CN) ₆] (7)	190	30	-190	10	380	5.3	0.98	155	55	14

^a Isotropic chemical shift $\delta_{\text{iso}} = (1/3)(\delta_{11} + \delta_{22} + \delta_{33})$. ^b Chemical shift span $\Omega = \delta_{11} - \delta_{33}$. ^c Nuclear quadrupolar coupling constant. ^d Asymmetry parameter of electric field gradient (EFG). ^e Euler angle.

**Figure 2.** The experimental and simulated ^{59}Co NMR spectra of complexes 1–4 at 300- and 400-MHz magnetic fields.

Computational Details. All calculations were performed by the Gaussian 94 package³¹ running on a SGI workstation. The hybrid B3PW91 functional (using Becke's three-parameter hybrid method and employing the Perdew 91 correlation functions)^{32,33} was used in all of the calculations as it has been demonstrated in general applications^{4,34} although the hybrid B3LYP functional has also been proven to be equally effective.⁵ All calculations were done with a 6-311+G* internal basis set which specifies the 6-311G basis for first-row atoms, the MacLean-Chandler (12s,9p)-(621111,52111) basis sets for second-row atoms,^{35,36} and the Wachters-Hay^{37,38} all-electron basis set for the first

(31) Frisch, M. J.; Trucks, G. W.; Schlegel, H. B.; Gill, P. M. W.; Johnson, B. G.; Robb, M. A.; Cheeseman, J. R.; Keith, T.; Petersson, G. A.; Montgomery, J. A.; Raghavachari, K. M.; Al-Laham, A.; Zakrzewski, V. G.; Ortiz, J. V.; Foresman, J. B.; Cioslowski, J.; Stefanov, B. B.; Nanayakkara, A.; Challacombe, M.; Peng, C. Y.; Ayala, P. Y.; Chen, W.; Wong, M. W.; Andres, J. L.; Replogle, E. S.; Gomperts, R.; Martin, R. L.; Fox, D. J.; Binkley, J. S.; Defrees, D. J.; Baker, J.; Stewart, J. P.; Head-Gordon, M.; Gonzalez, C.; Pople, J. A. *Gaussian 94, Revision B.2*, Gaussian Inc.: Pittsburgh, PA, 1995.

(32) Becke, A. D. *J. Chem. Phys.* **1993**, *98*, 5648.

(33) Perdew, J. P.; Wang, Y. *Phys. Rev.* **1992**, *B45*, 13244

(34) Baker, P.; Muir, M.; Andzelm, J. *J. Chem. Phys.* **1995**, *102*, 2063

(35) MacLean, A. D.; Chandler, G. S. *J. Chem. Phys.* **1993**, *98*, 5648–5652.

transition row, using the scaling factors of Raghavachari and Trucks³⁹ and augmented by polarization and diffuse functions.^{40,41}

The NMR shielding tensors were calculated by using the GIAO method⁴² and are given in parts per million relative to the absolute shielding of $[\text{Co}(\text{CN})_6]^{3-}$ ($\sigma_r = -5400$ ppm).^{5,43} Also, previous studies^{4b,5,44} have shown that the charge field effects are small toward the ^{59}Co isotropic, anisotropic, and absolute shieldings, as well as toward crystal-solution shifts. This finding suggests that the potassium ions in $\text{K}_3[\text{Co}(\text{CN})_6]$ can be neglected in the calculation. On the basis of the same rationale and also because of limited computational resources, the macro-rings of the supercomplexes 1–3 were not included in the calculations. The details of the NBO analysis employed in this work is referred to in our previous study.⁹ Accordingly, the results of the second-order perturbative analysis (SOPA), which is a module of the NBO package, are presented as a list of second-order interaction energies (E_2) between the natural bond orbitals of the donor and the acceptor.

The experimental geometries determined in our laboratory were used in all of the calculations. No symmetry elements at the Co sites were found for all of the supercomplexes in this study, and only one site was found for each supercomplex²¹ and for $\text{K}_3[\text{Co}(\text{CN})_6]$.⁴⁵

Results and Discussion

A. Charge-Transfer Mechanism Analysis. 1. Second-Sphere Interaction and Structure Distortion. Isotropic ^{59}Co Chemical Shifts and Bond Lengths. The Co–C, C≡N bond lengths and H-bond lengths for supercomplexes 1–3 as well as the Co–C, C≡N bond lengths for complex 4 are obtained from the available crystallographic data.^{21,45} To trace the relationships between the NMR parameters and structure distortions, the isotropic ^{59}Co chemical shifts have been plotted against the bond lengths of C≡N and Co–C as well as the averaged bond lengths of the H-bonds (Table 2). As shown in Figure 3A–C, the excellent correlations suggest that second-sphere interaction in the form of hydrogen bonding between the preorganized polyammonium macrocycles and $[\text{Co}(\text{CN})_6]^{3-}$ is the origin responsible for the structural distortion in $[\text{Co}(\text{CN})_6]^{3-}$. Further confirmation is readily derived from the observed weakening (lengthening)/strengthening (shortening) of

(36) Krishan, R.; Binkley, J. S.; Seeger, R.; Pople, J. A. *J. Chem. Phys.* **1980**, *72*, 650.

(37) Watchers, A. J. H. *J. Chem. Phys.* **1970**, *52*, 1033.

(38) Hay, P. J. *J. Chem. Phys.* **1977**, *66*, 4377.

(39) Raghavachari, K.; Trucks, G. W. *J. Chem. Phys.* **1989**, *91*, 1062.

(40) Clark, T.; Chandrasekhar, J.; Spitznagel, G. W.; Shleyer, P. V. R. *J. Comput. Chem.* **1983**, *4*, 294.

(41) Frisch, M. J.; Pople, J. A.; Binkley, J. S. *J. Chem. Phys.* **1984**, *80*, 3265–3269.

(42) (a) London, F. *J. Phys. Radium* **1937**, *8*, 397–409. (b) McWeeny, R. *Phys. Rev.* **1962**, *126*, 1028–1034. (c) Ditchfield, R. *Mol. Phys.* **1974**, *27*, 789–807. (d) Dodds, J. L.; McWeeny, R.; Sadlej, A. J. *Mol. Phys.* **1980**, *41*, 1419–1430. (e) Wolinski, K.; Hilton, J. F.; Pulay, P. *J. Am. Chem. Soc.* **1990**, *112*, 8251–8265.

(43) Bramley, R.; Brorson, M.; Sargeson, A. M.; Schäffer, C. E. *J. Am. Chem. Soc.* **1985**, *107*, 2780–2787.

(44) Eaton, D. R.; Bruist, R. J.; Sayer, B. G. *Can. J. Chem.* **1987**, *65*, 1332–1335.

(45) Zhou, P.; Xue, F.; Au-Yeung, S. C. F. *Acta Crystallogr.* **1998**, *C54*, 1833.

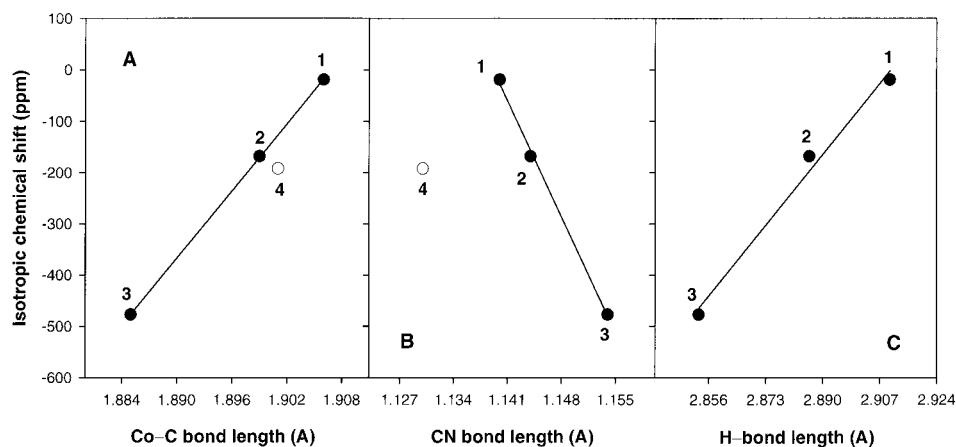


Figure 3. Correlation of experimental ^{59}Co isotropic chemical shifts with (A) Co–C bond, (B) C \equiv N bond, and (C) H-bond lengths.

Table 2. Average Co–C Bond, C \equiv N Bond, and H-bond Lengths

complex	Co–C (Å)	C \equiv N (Å)	H-bond (Å) ^a
[18]aneN ₆ [Co(CN) ₆] (1)	1.906	1.140	2.910
[16]aneN ₄ [Co(CN) ₆] (2)	1.899	1.144	2.886
[12]aneN ₄ [Co(CN) ₆] (3)	1.885	1.154	2.853
K ₃ [Co(CN) ₆] (4)	1.901	1.130	

^a Averages of the H-bonds were calculated by choosing all of the H-bonds except when two or more H-bonds attached to one nitrogen atom of a C \equiv N group, only the shortest H-bond was chosen.

the C \equiv N/Co–C bond which enhances the Co–C bond covalency,^{46,47} hence the observed upfield cobalt chemical shift. For K₃[Co(CN)₆] (4), because of the large radii of K⁺ ions compared with those of protons and the shorter distance (~ 2.95 Å)⁴⁵ between K⁺ and N of [Co(CN)₆]³⁻ (~ 4.13 Å in complex 1 and 4.04 Å in complex 2),²¹ Co and C are probably affected directly by the strong electrostatic interaction exerted by K⁺. Thus, a similar decrease in C \equiv N bond length is not expected for complex 4, that changes in the Co–C bond length will also be inconsistent with the trend observed for supercomplexes 1, 2, and 3.

^{59}Co Chemical Shift Tensor Components and Shift Span.

It has been well-established that deviation from cubic (O_h) nuclear site symmetry at Co in cobalt complexes would result in changes in the chemical shift tensor components, δ_{ii} ; the chemical shift span, Ω ; and the nuclear quadrupolar coupling constant, NQCC. The supercomplexes 1–3 and 5–7 uniquely contain [Co(CN)₆]³⁻ therefore providing a common comparative basis for obtaining insights into the response of the metal chemical shift tensor and shift span toward structure perturbation originating from second-sphere interactions. The X-ray²¹ and elemental analysis⁴⁸ results conclusively show that for supercomplexes 3, 6, and 7 there are no K⁺ ions in their structures, thereby eliminating electrostatic interaction through K⁺ as means of structure stabilization for these complexes. But for the

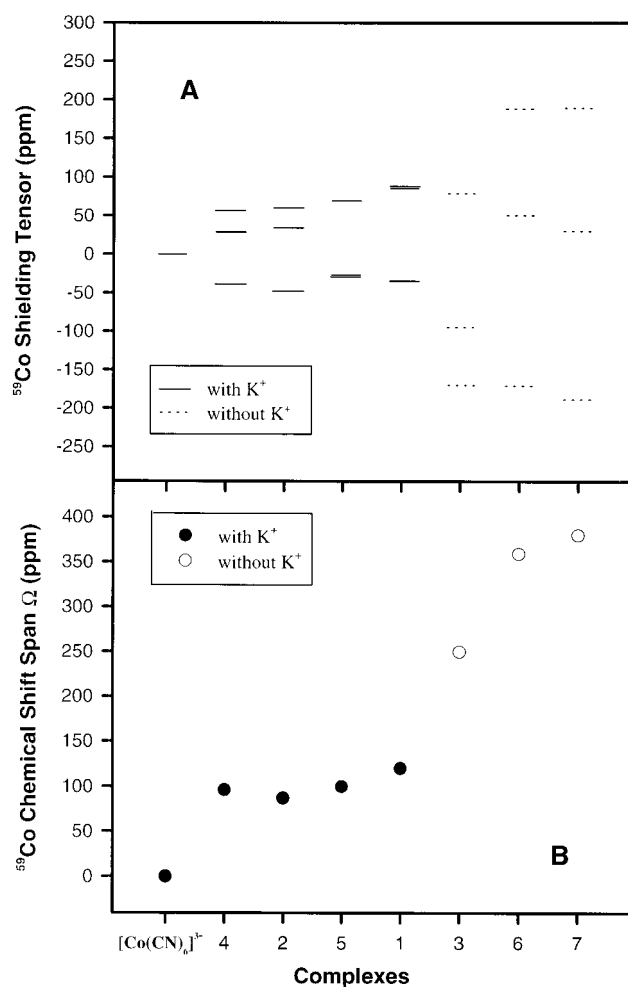


Figure 4. Variations of the (A) ^{59}Co chemical shielding components and (B) ^{59}Co chemical shift span Ω for complexes 1–7.

supercomplexes 1, 2, and 5 both electrostatic interaction with K⁺ and hydrogen bonding have been shown to coexist in the structures, whereas the structure of K₃[Co(CN)₆] (4) is stabilized by pure electrostatic interaction involving potassium. Figure 4A and B show the variation of the ^{59}Co chemical shift components and the shift span for these complexes. It is shown that Ω and the distribution of the δ_{ii} 's in structures without K⁺ ions are systematically larger than those containing potassium. This interesting result suggests that the hydrogen-bonding effect tends to exert a sizable influence in the distortion of the electronic environment at ^{59}Co , whereas K⁺ ions tend to disperse charge

(46) Mason, J. *Chem. Rev.* **1987**, *87*, 1299–1312.

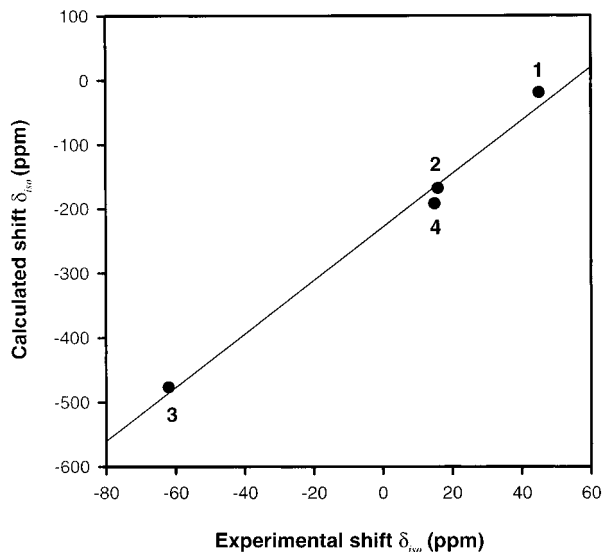
(47) Chan, J. C. C.; Au-Yeung, S. C. F. *J. Chem. Soc., Faraday Trans.* **1996**, *92*, 1121–1128.

(48) Elemental analysis results: [12]aneN₄[Co(CN)₆], formula C₈H₂₀N₄H₃[Co(CN)₆]·2H₂O, found C, 39.29; H, 6.34; N, 32.74; calcd C, 39.41; H, 6.40; N, 32.86. [18]aneN₆[Co(CN)₆], formula C₁₂H₃₀N₆H₂K[Co(CN)₆]·4H₂O, found C, 37.06; H, 6.83; N, 29.05; calcd C, 36.85; H, 6.87; N, 28.65. [24]aneN₈[Co(CN)₆], formula C₁₆H₄₀N₈H₆K₂[Co(CN)₆]·2Cl₂·6H₂O, found C, 32.22; H, 5.71; N, 27.25; calcd C, 32.59; H, 5.65; N, 27.15. [16]aneN₄[Co(CN)₆], formula C₁₂H₂₈N₄H₂K[Co(CN)₆], found C, 44.33; H, 6.12; N, 29.07; calcd C, 44.63; H, 6.20; N, 28.93. [24]aneN₆[Co(CN)₆], formula C₁₈H₄₂N₆H₆[Co(CN)₆]·5.5H₂O, found C, 41.23; H, 6.64; N, 28.42; calcd C, 41.05; H, 6.72; N, 28.73. [32]aneN₈[Co(CN)₆], formula C₂₄H₅₆N₈H₈[Co(CN)₆]·2Cl₂·6H₂O, found C, 40.26; H, 7.08; N, 26.10; calcd C, 40.11; H, 7.05; N, 26.10.

Table 3. Calculated and Experimental ^{59}Co Chemical Shifts, Shift Components (in the Traceless Representation), and Shift Spans (ppm)

complex	calcd						expt				
	δ_{11}^{TR}	δ_{22}^{TR}	δ_{33}^{TR}	δ_{iso}	δ_{iso}^a	Ω	δ_{11}^{TR}	δ_{22}^{TR}	δ_{33}^{TR}	δ_{iso}	Ω
[18]aneN ₆ [Co(CN) ₆] (1)	106	-22	-82	-19	219	188	41	39	-80	45	121
[16]aneN ₄ [Co(CN) ₆] (2)	66	-12	-53	-168	70	119	37	14	-51	16	88
[12]aneN ₄ [Co(CN) ₆] (3)	100	5	-105	-477	-239	205	142	-33	-109	-62	250
K ₃ [Co(CN) ₆] (4)	69	-5	-64	-192	46	133	38	21	-59	15	96

^a Related to the shielding intercept ($\sigma_r' = -5162$ ppm)²

**Figure 5.** Correlation between the calculated and experimental ^{59}Co isotropic chemical shifts δ_{iso} .

built up in localized regions in the structure, thus offsetting distortions induced by formation of hydrogen bonds. Of the three principal components, we also find δ_{22} to be linearly related with δ_{iso} . However, the origin of this correlation is unclear.

2. DFT Calculation of Chemical Shifts and Second-Order Interaction Energies (E_2). Recently, we and Oldfield et al. have independently demonstrated the use of hybrid XC-functional DFT method for the prediction of the isotropic ^{59}Co NMR chemical shifts of diamagnetic Co(III) complexes with a range of chemical shifts spanning $\sim 13\,000$ ppm.^{4b,5} However, the application of this method to the study of a series of complexes with similar constituents but small perturbation in structural or electronic environments that would result in small changes in the relative chemical shifts (i.e. differences of hundreds of ppm) has not been tested. To address this issue, we carry out the calculations of the chemical shift and shift tensor of the cobaltcyanide anion for supercomplexes **1–3** as well as that of K₃[Co(CN)₆]. Table 3 summarizes a comparison of the DFT calculation results and the solid-state NMR experimental results. The correlation of the calculated and experimental isotropic chemical shift is shown in Figure 5. Surprisingly, the agreement in the trend of the isotropic chemical shifts could be considered excellent for a small chemical shift range of <700 ppm when taking into consideration medium effect (~ 300 ppm)^{4b,49} and when the value of absolute shielding $\sigma_r = -5400$ ppm⁴³ has been replaced by the shielding intercept of cobalt ($\sigma_r' = -5162$ ppm) determined by Oldfield et al.⁵ A fair trend is also observed between the calculated chemical shift span Ω and the experimental values (Table 3, column 7 and 12). Therefore, it is demonstrated that hybrid XC-functional DFT method has been successfully applied to the calculation of ^{59}Co .

(49) Taura, T. *Bull. Chem. Soc. Jpn.* **1990**, *63*, 1105 and references therein.

Co chemical shift and shift (shielding) tensor components not only for shifts spanning a large shielding range ($\sim 13\,000$ ppm, different Co(III) complexes)^{4,5} but also for shifts spanning smaller changes in shielding properties (~ 700 ppm, similar Co(III) complexes).

To better understand the charge-transfer mechanism in the self-assembled [Co(CN)₆]³⁻ and the preorganized protonated polyammonium macrocyclic cations, the relative contribution of cobalt-3d orbitals to second-order interaction energies, E_2 , is investigated on the basis of eq 3.

$$E_2(C_i \rightarrow 3d)\% = \frac{\sum_{i=1}^6 E_2\{\text{LP}(C_i, sp^n) \rightarrow \text{LP}^*(\text{Co}, 3d)\}}{\sum_{i=1}^6 E_2\{\text{LP}(C_i, sp^n) \rightarrow \text{LP}^*(\text{Co}, 3d)\} + \sum_{i=1}^6 E_2\{\text{LP}(C_i, sp^n) \rightarrow \text{LP}^*(\text{Co}, 4s)\}} \times 100\% \quad (3)$$

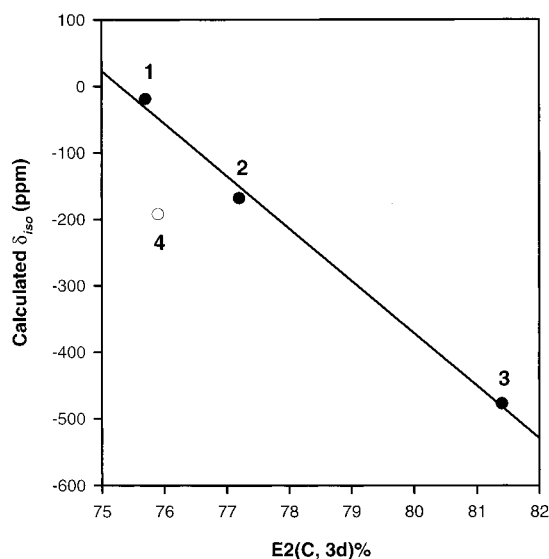
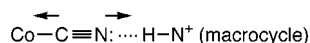
The entry $\text{LP}(C_i, sp^n)$ indicates a sp^n ($n = 0.76–0.78$ for this work) hybridized NBO orbital of the carbon atom C_i which accommodates a lone pair of electrons while the entries $\text{LP}^*(\text{Co}, 3d)$ and $\text{LP}^*(\text{Co}, 4s)$ describe an antibonding NBO orbital of cobalt which is comprised of pure cobalt-3d orbitals and -4s orbitals, respectively. The interaction energy (E_2) obtained using the SOPA routine of the NBO package, which reveals the extent of the charge transferred from the ligand (C_i) to cobalt for **1**, **2**, **3**, and **4**, are summarized in Table 4. In this study, only contributions from the cobalt-3d and -4s orbitals are considered as the total second order interaction energies because other orbital contributions to E_2 are relatively small.⁵⁰ For these complexes, the SOPA results indicate the dominating role of the Co-3d orbital (Co-3d contribution $>75\%$).

Note that the calculated ^{59}Co isotropic chemical shifts (δ_{iso}) correlates well with the averaged Co-3d second-order interaction energy contribution, $E_2(C \rightarrow 3d)\%$, for the three supercomplexes (Figure 6). In a previous study⁹ of the pentaamminecobalt(III) complexes, we have shown that the covalence of the cobalt-ligand interaction is directly proportional to the extent of the Co-3d orbital participation. Within the framework of the hard and soft acid–base concept, increasing covalent character in the Co-ligand bond would be interpreted as increases in cobalt-3d electron delocalization to the ligand X, which diminishes the magnitude of the 3d-orbital radial factor, $\langle r^{-3} \rangle_{3d}$ and therefore causes an upfield shift of the ^{59}Co chemical shift.^{46,47} The $\delta_{\text{iso}}(^{59}\text{Co})$ and $E_2(C \rightarrow 3d)\%$ correlation presented here conclusively supports this interpretation. Furthermore, the dependence of $E_2(C \rightarrow 3d)\%$ on the Co–C bond lengths and C≡N bond lengths, as well as on the hydrogen bond lengths (Figures 7A–C) confirms that hydrogen-bonding interaction is responsible for these correlations.

(50) Less than 5%.

Table 4. Relative Contribution of Cobalt 3d Orbitals to Second-Order Interaction Energy (E_2)

complex	$E_2(C_1 \rightarrow 3d)\%$	$E_2(C_2 \rightarrow 3d)\%$	$E_2(C_3 \rightarrow 3d)\%$	$E_2(C_4 \rightarrow 3d)\%$	$E_2(C_5 \rightarrow 3d)\%$	$E_2(C_6 \rightarrow 3d)\%$	ave. $E_2(C \rightarrow 3d)\%$
[18]aneN ₆ [Co(CN) ₆] (1)	75.3	75.9	76.2	75.6	76.2	75.4	75.8
[16]aneN ₄ [Co(CN) ₆] (2)	76.9	77.8	77.8	76.2	77.0	77.3	77.2
[12]aneN ₄ [Co(CN) ₆] (3)	81.0	80.9	82.0	82.7	80.7	80.8	81.4
K ₃ [Co(CN) ₆] (4)	76.3	76.0	75.4				75.9

**Figure 6.** Dependence of the calculated ⁵⁹Co isotropic chemical shifts (δ_{iso}) on the averaged Co 3d contribution ($E_2(C \rightarrow 3d)\%$).**Scheme 1****3. Charge-Transfer Model and Bond Length Variation**

Rules. On the basis of the evidences presented, the charge-transfer mechanism involving hydrogen-bonding interaction between $[\text{Co}(\text{CN})_6]^{3-}$ and polyammonium macrocycles may be described as depicted in Scheme 1.

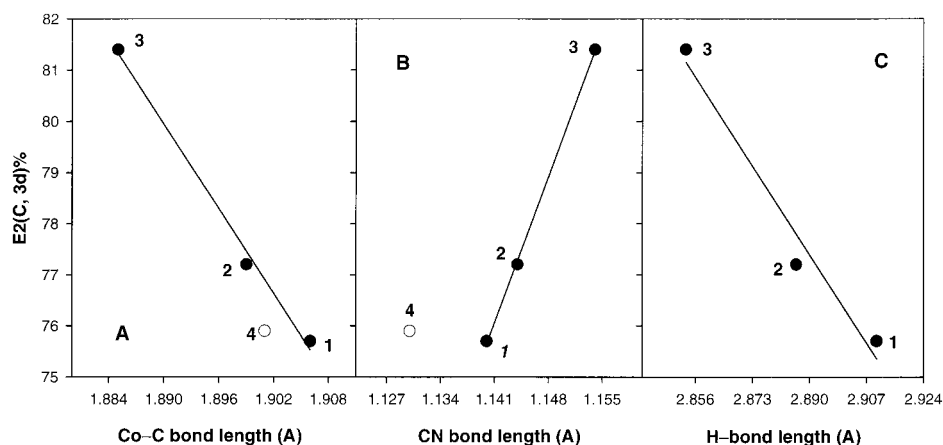
That is, the formation of the hydrogen bond induces the charge transfer from nitrogen to the preorganized second-sphere ligand, causing charge separation across the $\text{C}\equiv\text{N}$ bonds, thus increasing the charge density localized on the carbon atom. Consistent with Gutmann's bond length variation rule, these effects induce charge transfer to Co that would enhance the covalent character of the metal–ligand interaction, thereby strengthening the Co–C bond. Since the increase in the Co–C covalence is achieved by an increase in the contribution of the 3d orbital participation,⁹ there is, consequently, an upfield shift

of the ⁵⁹Co chemical shift.⁴⁷ Therefore, the origin responsible for the charge-transfer process in supercomplexes and the relationship between the changes in Co–C and $\text{C}\equiv\text{N}$ bond lengths and that of hydrogen-bonding interaction is readily revealed.

B. Photochemical Property and Structure Distortion Correlation. If structure distortion resulting from second-sphere interaction is responsible for the modification in the photochemical property of the supercomplexes **6** and **7**, an analysis of their ⁵⁹Co chemical shift components within the framework of the strong field approximation⁵¹ of the Ramsey shielding equation⁵² would directly reveal insights into their relationship with the energy structure at Co (also see Appendix I). Accordingly, the energy splitting Δ_{ES} (in wavelength) between the highest and the lowest energy states is related to Ω by eq 4

$$\begin{aligned} \Delta_{\text{ES}} &= \lambda_3 - \lambda_1 \approx (-1/K_\lambda)(\sigma_{33}^{\text{P}} - \sigma_{11}^{\text{P}}) \\ &= (1/K_\lambda)(\delta_{11} - \delta_{33}) = (1/K_\lambda)\Omega \end{aligned} \quad (4)$$

Using eq A4 (Appendix I), K_λ is determined to be 24.14 ppm·nm⁻¹ on the basis of the known absolute chemical shielding value of $[\text{Co}(\text{CN})_6]^{3-}$ (–5400 ppm),⁴³ the calculated diamagnetic shielding value of ⁵⁹Co (2155 ppm),^{4a} and the value of the dissociation energy (31949 cm⁻¹) corresponding to 313 nm. The calculated maximum energy splittings are 3.9, 14.9, and 15.7 nm corresponding to ⁵⁹Co chemical shift spans of 96, 359, and 380 ppm for $[\text{Co}(\text{CN})_6]^{3-}$, [24]aneN₆[Co(CN)₆], and [32]aneN₈[Co(CN)₆], respectively. On the basis of these estimates and the reported light bandwidth¹¹ (~12 nm) used in the photochemical experiments, it is plausible that excitations of excited states resulting from the splitting of the ¹T_{1g} state are partially covered by this bandwidth. Only the central band at 313 nm may produce electron excitation with maximum efficiency. Therefore, there appears to be maximum excitation efficiency for “free” $[\text{Co}(\text{CN})_6]^{3-}$ because its energy states are very close to being triply degenerate. For [24]aneN₆[Co(CN)₆] and [32]aneN₈[Co(CN)₆], the excitations of the first and the third excited states are away from the central band (313 nm); hence, lower excitation efficiency (lower excitation ratios) is achieved in their irradiation. This effect may result in lower photoaquation

**Figure 7.** Relationship of the averaged Co 3d contribution ($E_2(C \rightarrow 3d)\%$) with (A) Co–C bond, (B) $\text{C}\equiv\text{N}$ bond, and (C) H-bond lengths.

quantum yield especially the frequency span line shape for a Hg lamp is generally not square. Also, the gain in the enhancement in Co–C covalence due to hydrogen bonding may partially contribute to the reduction in photoaquation quantum yield. No obvious change was observed in the absorption spectra.¹¹ This could be readily understood because the sum weighted average transition energies of the nondegenerate states in [24]aneN₆[Co(CN)₆] and [32]aneN₈[Co(CN)₆] are comparable to the ¹T_{1g} energy of free cobaltcyanide and the small shift in the energies between the ground and the three nondegenerate states could not be resolved into three individual transitions in the optical spectrum.

Conclusions

The charge-transfer mechanism in the hydrogen-bonding interaction for a series of preorganized protonated polyammonium macrocycle cobaltcyanide supercomplexes has been established through a study of solid-state ⁵⁹Co NMR and DFT calculation. The correlation between the ⁵⁹Co chemical shifts, the relative contribution of cobalt-3d orbitals to second-order interaction energies, as well as the conformational parameters, confirmed that structure distortions in these supercomplexes are the direct consequence of the second-sphere interaction. It has been confirmed that structure distortion removes the degeneracy of the triply degenerate electron energy state (¹T_{1g}) at cobalt, causing splitting in the energy levels. In short, the spectrochemical properties of these supercomplexes have been slightly modified which is revealed experimentally through ⁵⁹Co NMR tensor measurements. In addition, it has also been demonstrated that an entire ⁵⁹Co chemical shift range may be predicted with reasonable confidence using ab initio method at DFT level.

The results presented in this study have shown that combined DFT and solid-state NMR methods could have strong developmental potential for the study of the molecular structure and the electronic property of polycrystalline materials involving transition metals.

Acknowledgment. This research is supported by a RGC Earmarked Research Grant (CUHK 312/94P). We are grateful for a grant supporting the purchase of the ASX-300 NMR spectrometer by the Research Grants Council of Hong Kong Special Administrative Government under the Central Allocation Scheme (1992). We are indebted to Prof. Wasylishen at Dalhousie University, Canada, for making the AMX 400 NMR spectrometer facility available for recording the spectra. We also thank Dr. Jerry C.C. Chan for helpful discussions and assistance in making the measurements on the AMX 400 NMR spectrometer.

(51) (a) Freeman, R.; Murry, G. R.; Ricards, R. E. *proc. R. Soc. London, Ser. A*, **1957**, 53, 601. (b) Griffith, J. S.; Orgel, L. E. *Trans. Faraday Soc.*, **1957**, 53, 601.

(52) Ramsey, N. F. *Phys. Rev.* **1950**, 78, 699.

Supporting Information Available: One figure showing the experimental and simulated solid-state NMR spectra of supercomplexes **5–7** at two magnetic fields and four tables listing the detailed SOPA results of these complexes (3 pages, print/PDF). See any current masthead page for ordering and Internet access instructions.

Appendix I

For diamagnetic d⁶ complexes in a strong octahedral ligand field, the paramagnetic shielding term, which is the major effect responsible for the metal NMR chemical shift, can be described by the strong field approximation of the Ramsey shielding equation

$$\sigma_{\text{iso}}^{\text{p}} = -\frac{8\mu_0\mu_B^2\langle r^{-3} \rangle_{3d}|\langle {}^1A_{1g}|L_z|{}^1T_{1g} \rangle|^2}{\pi\Delta E_{({}^1A_g-{}^1T_g)}} \quad (\text{A1})$$

In eq A1, the symbols carry their usual meaning. Equation A1 may be rewritten in the form

$$\sigma_{\text{iso}}^{\text{p}} = -B_0\eta/\Delta E \quad (\text{A2})$$

where B_0 is a constant, and η is the covalence factor which has a value close to the nephelauxetic β_{35} . When the degeneracy of the ¹T_{1g} state is removed, the cubic symmetry of Co in [Co(CN)₆]³⁻ has been lifted causing a splitting of the ¹T_{1g} state. As a result, the chemical shielding constant splits into the corresponding tensor components σ_{11} , σ_{22} , and σ_{33} , and the energy splitting of ¹A_{1g} → ¹T_{1g} is resolved into ΔE_1 , ΔE_2 , and ΔE_3 accordingly. That is,

$$\begin{aligned} \sigma_{\text{iso}}^{\text{p}} &= (1/3)(\sigma_{11}^{\text{p}} + \sigma_{22}^{\text{p}} + \sigma_{33}^{\text{p}}) \\ &= (-B_0/3)[(\eta_1/\Delta E_1) + (\eta_2/\Delta E_2) + (\eta_3/\Delta E_3)] \end{aligned} \quad (\text{A3})$$

In eqn A3, ΔE_i is the transition energy from ¹A_{1g} to the i th excitation state. Assuming η_i 's are approximately the same for this type of system, the expression A3 could be manipulated to give

$$\sigma_{ii}^{\text{p}} \approx -K/\Delta E_i = -K_\lambda\lambda_i \quad (\text{A4})$$

and

$$\sigma_{\text{iso}}^{\text{p}} = -(1/3)K(1/\Delta E_1 + 1/\Delta E_2 + 1/\Delta E_3) = -K'/\Delta E$$

or

$$\sigma_{\text{iso}}^{\text{p}} = -(1/3)K_\lambda(\lambda_1 + \lambda_2 + \lambda_3) = -K_\lambda\lambda \quad (\text{A5})$$

JA981924D